Polarization of Σ^+ Hyperons Produced by 400-GeV Protons

C. Wilkinson, R. Handler, B. Lundberg, L. Pondrom, and M. Sheaff
Physics Department, University of Wisconsin, Madison, Wisconsin 53706

and

P. T. Cox, C. Dukes, J. Dworkin, and O. E. Overseth
Department of Physics, University of Michigan, Ann Arbor, Michigan 48109

and

A. Beretvas, L. Deck, T. Devlin, K. B. Luk, R. Rameika, and R. Whitman
Physics Department, Rutgers—The State University, Piscataway, New Jersey 08854

and

K. Heller
Physics Department, The University of Minnesota, Minneapolis, Minnesota 55455

The polarization of 26 000 Σ^+ hyperons produced by 400-GeV protons on Be has been measured. The polarizations of Σ^+ and Λ hyperons have the opposite sign. The magnitude increases with momentum at 5-mrad production angle, and averages 22% over the momentum range 140 to 280 GeV/c.

This Letter reports the first observation of polarization in high-energy charged-hyperon production. A short positive 200-GeV/c secondary beam produced by 400-GeV protons incident on a beryllium target contained Σ^+ hyperons which were detected via the decay $\Sigma^+ \rightarrow p\pi^0$. Preliminary data reported here show that the polarization is comparable in magnitude, but opposite in sign, to that previously observed for Λ's.[1] The sign change is anticipated by a simple quark-model picture of the production reaction.[2]

The experiment was performed in the $M2$ beam at Fermilab. A schematic view of the apparatus is shown in Fig. 1. A series of bending magnets permitted steering of the proton beam onto the one-half interaction-length Be target at angles of $+5$ or -5 mrad in the vertical plane. Parity-conserving polarization was defined to be positive in the direction $\vec{k}_p \times \vec{k}_\Sigma$, where $\vec{k}_p$ and $\vec{k}_\Sigma$ were the incident proton and outgoing Σ^+ momenta. This vector pointed along $+x$ for $+5$ mrad. A vertical magnetic field (parallel to $-y$) steered the charged beam through a 5.3-m-long curved channel. The field integral was 6.6 T m. A central ray through the collimator was bent 10 mrad, corresponding to 200 GeV. The particle flux transmitted by the channel had momenta between 140 and 280 GeV/c.

The detector was the basic multiwire proportional chamber (MWPC) spectrometer used in the neutral-beam experiment,[3] augmented by a scintillation counter $S1$, a set of three drift chambers ($D1 - D3$), and two MWPC's ($C1$, $C2$) located upstream. These served to detect the $\Sigma^+ \rightarrow p\pi^0$ decay vertex and to measure the Σ^+ momentum from its trajectory through the channel. The daughter proton momentum was measured in the downstream spectrometer (MWPC's $C3-C5$, bending magnets $C6-C8$). A lead-glass array at the back of the spectrometer detected at least one γ ray from π^0 decay.

The trigger selected events in which a high-momentum, positively charged particle passed through the upstream detectors and the spectrometer, accompanied by a signal in the lead-glass counters. The charged track signature was $S = S1 \cdot C3 \cdot PC$. The gamma trigger (GOR) required a pulse height from the summed lead-glass counters corresponding to a shower energy greater than 3 GeV. Triggers from charged particles striking the glass were prevented by the veto counter (T). The full event trigger coincidence was $\Sigma = S \cdot GOR \cdot T$. A small fraction (1/1024) of particles with only the S signature was mixed into the event trigger in order to obtain a sample of beam tracks.

Data at one production angle were taken under stable conditions for about four hours (2 tapes of ~52 000 triggers each), after which the production angle was reversed and the process repeated. The beam intensity was kept at a level compatible with high, stable drift-chamber efficiency. This
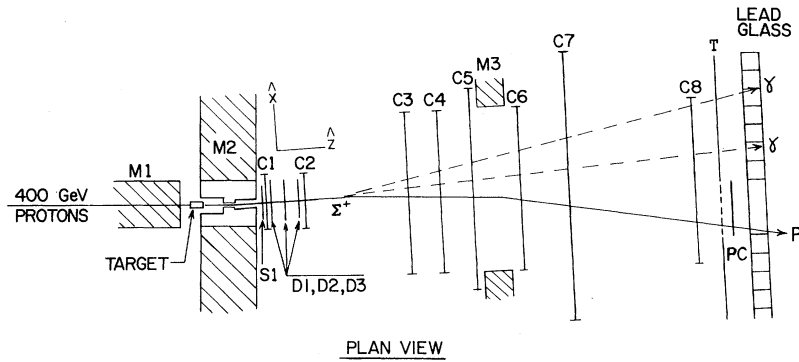
PLAN VIEW

FIG. 1. Schematic of the charged-hyperon beam in plan view. Magnet $M1$ deflected the protons into the target in the vertical plane. The magnet $M2$, the one used in Ref. 1 to define a neutral beam, formed a charged beam by a 10-mrad bend in the horizontal plane. This magnet was 5.3 m long, with a defining hole 4 mm in diameter in a tungsten plug 3 m from the target. The X-Z coordinate axes rotated with the charged beam. The Z positions of the upstream detector components were: $S1$ at 0 m; $C1$ at 0.67 m; $D1$ at 0.92 m; $D2$ at 2.71 m; $D3$ at 4.54 m; $C2$ at 5.06 m; and $C3$ at 13.18 m. The rest of the spectrometer was essentially the same as in Ref. 1. The aperture of the analyzing magnet $M3$ was 0.6 m (horizontal) $\times$ 0.2 m (vertical). At the back of the apparatus decay protons were counted in the 10×30 cm^2 scintillator PC (proton counter). The protons then passed through a hole in the lead-glass counter. T was a large veto scintillator to reject charged particles which hit the glass. There were no lead-glass blocks directly behind PC. The total length from $S1$ to the lead-glass counter was 40 m.

corresponded to about 1.5×10^9 protons per pulse on the beryllium target, and 2×10^5 charged tracks through the upstream part of the apparatus. About 0.5% of the positively charged beam after the magnetic channel was Σ^+ hyperons. The horizontal and vertical position of the beam on the production target were carefully maintained at optimum for each production angle. Approximately 2 800 000 triggers were collected, of which 6% could be reconstructed and identified as Σ^+. The data used for this report comprise 18% of the total sample. Matched pairs of tapes for +5- and −5-mrad production-angle data were selected at intervals from the whole data set.

Only the charged-track information was used for this analysis. A geometric fitting program searched for a single, positively charged track through the spectrometer with a kink between $D1$ and $C3$. Typical kink angles were ~1 mrad, measured with a resolution of 0.25 mrad full width at half maximum (FWHM). Events were also fit to a "no-kink" hypothesis and those which fit this hypothesis were classified as beam tracks and rejected. The momentum of the Σ^+ was determined by fitting the tentative Σ^+ track through the curved collimator with the target and the collimator apertures as constraints, with a resulting $\Delta p/p = 8\%$ FWHM. Figure 2 shows the invariant mass computed under the hypothesis that the positive decay product is a proton and the missing neutral is a π^0.

Beam particles in accidental coincidence with γ rays which fitted the $\Sigma^+ \to p$ decay hypothesis
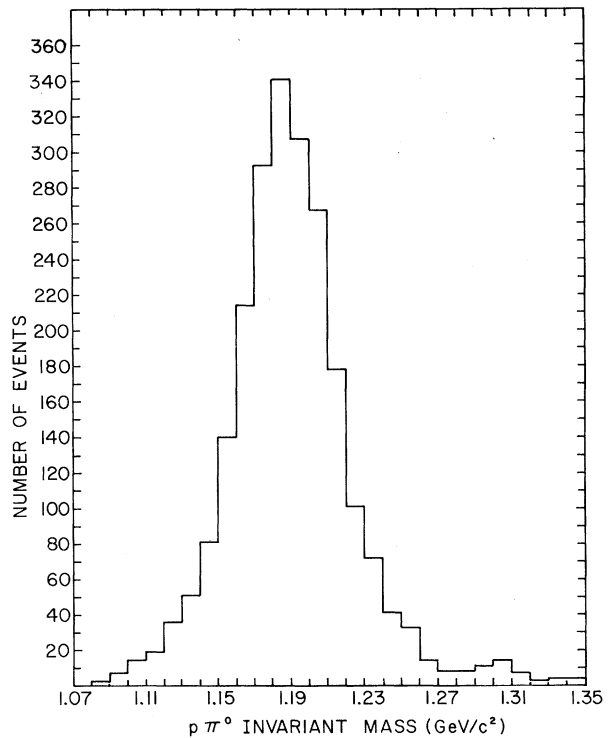
FIG. 2. The $p\pi^0$ invariant-mass plot obtained from the measured values of $\vec{p}_p$ and $\vec{p}_\Sigma$:

$$M^2 = \{(p_p{}^2 + m_p{}^2)^{1/2} + [\,(\vec{p}_\Sigma - \vec{p}_p)^2 + m_\pi{}^2]^{1/2}\}^2 - p_\Sigma{}^2.$$

804

and $K^+ \rightarrow \pi^+\pi^0$ decays were the major sources of background. Beam tracks were fitted to the Σ^+ $\rightarrow p$ hypothesis, and the yield of successful events when combined with the γ accidental rate gave a 3% background from this source. The K^+ decay was suppressed by the long lifetime, and contributed about 2% background. No corrections have been made to the results for possible background effects.

A full kinematic fit was performed to the hypothesis $\Sigma^+ \rightarrow p\gamma^0$ with the Σ^+ mass as a constraint. From the parameters of this fit, the direction cosines of the proton momentum in the Σ^+ rest system were computed along the local coordinate axes: $\hat{z}$ parallel to the Σ^+ laboratory momentum, $\hat{y} \perp \hat{z}$ in the vertical plane, and $\hat{x} = \hat{y} \times \hat{z}$ (horizontal). The Σ^+ polarization $\vec{P}$ was determined by the asymmetry in the angular distribution of the daughter protons along each of these axes.

The event distribution in the x direction cosine was expressed as

$$R_x^{\pm}(\cos\theta_i) = (\tfrac{1}{2}\Delta)A_x(\cos\theta_i)(1 \pm \alpha_\Sigma P_x \cos\theta_i), \quad (1)$$

with similar equations for the y and z components. Here the $\pm$ signs refer to ± 5-mrad production, $\alpha_\Sigma = -0.979 \pm 0.016$,[4] $\cos\theta_i$ is histogrammed in twenty equal bins of width $\Delta = 0.1$ (larger than the average resolution $\Delta \cos\theta = 0.05$ FWHM), and $A_x(\cos\theta_i)$ is the acceptance of the apparatus. The acceptance depended on the component x, the $\cos\theta_i$ bin, and the Σ^+ momentum. It was normal-

ized to unity over the range $-1 < \cos\theta_i < +1$. The acceptance in $\cos\theta_z$ averaged over Σ^+ momentum was flat for $-0.9 \lesssim \cos\theta_z \lesssim +0.5$, with the forward-direction $\cos\theta_z > 0.5$ depleted to about 60% of the full value. The distortion in $\cos\theta_x$ was less severe. For each bin $\cos\theta_i$ the asymmetry was calculated from the ratio

$$\alpha_\Sigma P_x \cos\theta_i = \frac{R_x^{+}(\cos\theta_i) - R_x^{-}(\cos\theta_i)}{R_x^{+}(\cos\theta_i) + R_x^{-}(\cos\theta_i)}, \quad (2)$$

and then a least-squares fit was performed to determine the best value of $\alpha_\Sigma P_x$. This technique cancelled effects due to acceptance biases. The data were divided in 20-GeV/c-wide Σ^+ momentum bins between 140 and 280 GeV/c. The ratio defined by Eq. (2), averaged over all momenta, is plotted in Fig. 3. The momentum averages of the three components of the polarization and their statistical errors are $\alpha_\Sigma P_x = 0.215 \pm 0.011$, $\alpha_\Sigma P_y = -0.035 \pm 0.011$, and $\alpha_\Sigma P_z = -0.011 \pm 0.011$. The result for $\alpha_\Sigma P_z$, which should vanish within the errors, gives an indication of the systematic uncertainty.

The vector $\vec{P}$ determined by these components must then be corrected for precession in the field of $M2$. Using $\mu_\Sigma = 2.33 \pm 0.13$ nuclear magnetons as the Σ^+ magnetic moment,[5] the angle between $\vec{P}$ and the Σ^+ momentum vector $\vec{k}_\Sigma$ should change by $186° \pm 16°$. Rotating $\vec{P}$ by this amount gave the polarization vector at the production target, which was along the direction $\vec{k}_p \times \vec{k}_\Sigma$ within statistical uncertainties. A systematic uncertainty of ± 0.05 was combined in quadrature with each statistical error. The values of $\vec{P}_0$ as

FIG. 3. The measured ratio $\alpha_\Sigma P_x \cos\theta_i$ vs $\cos\theta_i$ as defined by Eq. (2) for all Σ^+ data with 140 GeV/c $\leq p_\Sigma$ ≤ 280 GeV/c. The slope of the solid line is αP_x for the total data sample. This asymmetry was observed after precession through $186° \pm 16°$ in the magnetic channel, which explains the sign difference between P_x here (negative) and P_x at the production target in Fig. 4 (positive).
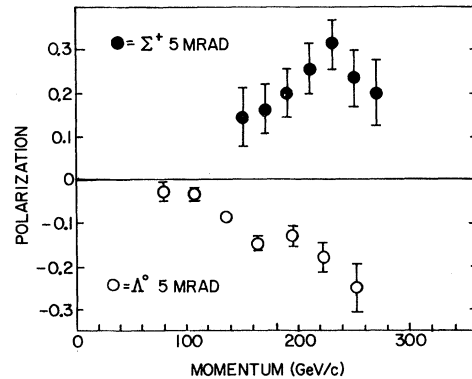
FIG. 4. Polarization of Σ^+ hyperons vs laboratory momentum for 5-mrad production. The sign choice is $+\vec{P}_\Sigma$ in the direction of $\vec{k}_p \times \vec{k}_\Sigma$. The 5-mrad Λ polarization data from Ref. 6 are plotted for comparison. The observed polarizations are opposite in sign and approximately equal in magnitude.

a function of p_Σ, the momentum of the Σ^+, are plotted in Fig. 4, along with comparable data for Λ.[6] The magnitude of the Σ^+ polarization is the same as that of the Λ at the same momentum. The most remarkable feature of this new data is that the sign of the polarization is opposite that of Λ.

The simple quark model referred to above assumes that one quark in the incident proton is lost through a hard collision, leaving a spectator diquark (uu or ud) which then picks up an s quark to form the forward out-going hyperon. Thus $uud \rightarrow uus$ produces a Σ^+, while $uud \rightarrow uds$ produces either a Λ or a Σ^0. Assume that the s quark is polarized by some unspecified mechanism. Then $P_\Lambda = P_s$, because the (ud) spectator is in a singlet state. For the Σ^+ and Σ^0 the nonstrange quarks must be in a triplet state, so that the polarization of the composite baryon is opposite to that of the strange quark: $P_{\Sigma^+} = P_{\Sigma^0} = -\frac{1}{3}P_\Lambda$. The observed sign reversal is thus expected from the model,

although the predicted magnitude $|P_{\Sigma^+}| = \frac{1}{3}|P_\Lambda|$ is smaller than the measured one.

[1]K. Heller et al., Phys. Rev. Lett. 41, 607 (1978).
[2]The model is discussed in Ref. 1. See also B. Andersson et al., Phys. Lett. 85B, 417 (1979).
[3]P. Skubic et al., Phys. Rev. D 18, 3115 (1978).
[4]R. L. Kelly et al. (Particle Data Group), Rev. Mod. Phys. 52, No. 2, Pt. 2, S1 (1980). This number is the average of several experiments.
[5]R. Settles et al., Phys. Rev. D 20, 2154 (1979).
[6]L. C. Schachinger, Ph.D. thesis, Rutgers University, 1978 (unpublished).

Construction of Exact Yang-Mills-Higgs Multimonopoles of Arbitrary Charge

M. K. Prasad
Department of Mathematics, Massachusetts Institute of Technology, Cambridge, Massachusetts 02139

and

P. Rossi[a]
Center for Theoretical Physics, Laboratory for Nuclear Science and Department of Physics,
Massachusetts Institute of Technology, Cambridge, Massachusetts 02139
(Received 12 December 1980)

Exact axially symmetric multimonopole solutions of arbitrary topological charge are presented and their relevant features discussed.

Ever since the pioneering work of 't Hooft and Polyakov[1] there has been considerable interest in static finite-energy magnetic-monopole solutions of classical Yang-Mills-Higgs gauge theories. More than five years ago, in the limit of vanishing Higgs potential, an exact analytic charge-one monopole solution was discovered.[2] Since then many people have tried, unsuccessfully, to find exact analytic multimonopole solutions. However, recently Ward[3] made a major breakthrough by presenting for the first time an exact analytic charge-two monopole solution. Inspired by Ward's work, we have now constructed, for the first time, exact monopole solutions of arbitrary charge. It is this construction we wish to describe in this

Letter. The calculations leading to our construction will be briefly sketched. The details are quite involved and are presented elsewhere.[4]

Let us define in four-dimensional Euclidean space (x_1, x_2, x_3, x_4) the SU(2) gauge potentials $A_\mu{}^a$ when $a = 1, 2, 3$ and $\mu = 1, 2, 3, 4$. The gauge field strength is defined by

$$F_{\mu\nu}{}^a \equiv \partial_\mu A_\nu{}^a - \partial_\nu A_\mu{}^a + \epsilon^{abc} A_\mu{}^b A_\nu{}^c. \tag{1}$$

Multimonopole solutions, with magnetic charge $n = 1, 2, 3, \ldots$, may be found[5,6] within the framework described in Refs. 5 and 6. This means we want to solve the self-duality equations:

$$F_{\mu\nu}{}^a = \frac{1}{2}\epsilon_{\mu\nu\rho\sigma}F_{\rho\sigma}{}^a \tag{2}$$